AIAA JOURNAL
Vol. 49, No. 12, December 2011

Discretization Error Estimation in Multidisciplinary Simulations

Sirisha Rangavajhala,* Venkata S. Sura,† Vadiraj K. Hombal,* and Sankaran Mahadevan‡
Vanderbilt University, Nashville, Tennessee 37205

DOI: 10.2514/1.J051085

This paper proposes methods to estimate the discretization error in the system output of coupled multidisciplinary simulations. In such systems, the governing equations for each discipline are numerically solved by a different computational code, and each discipline has different mesh size parameters. A classic example of multidisciplinary analysis involves fluid–structure interaction, where the element sizes in fluid and structure meshes are typically different. The general case of three-dimensional steady-state problems is considered in the current paper, where mesh refinement is possible in all three spatial directions for each discipline. Two aspects of discretization error, which are of interest in multidisciplinary analysis, are considered: disciplinary mesh sizes and the mismatch of disciplinary meshes at the interface at which boundary conditions are exchanged. Two alternate representations for the discretization error for the previously specified generic case are presented: 1) ignoring mesh mismatch at the interface and 2) considering mesh mismatch at the interface. Polynomial, rational function, and Gaussian process error models are used to represent the discretization error. The proposed error models are illustrated using a three-dimensional fluid–structure interaction problem of an aircraft wing.

I. Introduction

LARGE-SCALE systems (e.g., aircraft and automobiles) typically consist of subsystems of several disciplines, each governed by different physics (e.g., structural dynamics, fluid dynamics, acoustics, heat transfer, and control). Physics-based computer simulation models are typically built for individual disciplines to yield disciplinary outputs, which are computationally expensive by themselves. Appropriately accounting for the interactions among subsystems, either feedback or feedforward, adds to the computational expense of obtaining a system-level output. A common example of multidisciplinary analysis (MDA) is the simulation of the fluid–structure interaction (FSI) of an aircraft wing, where the structural analysis and the fluid analysis are coupled with each other. Such aeroelastic analyses form an essential component of design of aerospace vehicles [1–3].

It is well known that computational models, however sophisticated, are simplified representations of reality and are built by making several assumptions and simplifications. Verification, validation, and error estimation of computational models are topics of active research [4–6]. Rebba et al. [4] classify model errors into two major categories: model form error and numerical solution error. Model form error arises because of wrong or simplifying assumptions about system behavior, operating conditions, model parameters, and inputs. Examples of numerical solution errors include input errors, discretization errors [e.g., in finite element analysis (FEA)], and truncation errors (e.g., lower-order approximations). Discretization error is a critical component of numerical solution errors; this arises due to the solution of a continuum problem (typically characterized by partial differential equations) through finite element or finite difference solution methods that discretize the continuous domain.

This paper focuses on computational models of coupled multidisciplinary systems and the discretization error estimation of such systems. Simulation models for such systems usually have different mesh controls for each discipline. Moreover, most realistic problems have three-dimensional (3-D) geometries, with possible mesh refinement in all three spatial directions. The disciplinary meshes may not often match topologically (as discussed later), and this may additionally contribute to discretization error. In the following paragraphs, a brief overview is provided of the existing discretization estimation methods in the literature and their applicability for MDA.

A posteriori error estimation [7] for finite element methods is an active field of research. Ainsworth and Oden [8] present an extensive discussion of this topic. A posteriori methods typically use the solution of the finite element mesh to estimate the solution errors. In addition to computing the global error in the energy norm for a given mesh, recent advances in a posteriori methods also facilitate goal-oriented error estimation [9], i.e., error estimation in specific functionals of interest (e.g., lift and drag). A posteriori methods also facilitate adaptive mesh refinement schemes.

Richardson extrapolation [10,11] is a simple and useful technique to estimate discretization errors. Let f_{true} be the true solution of the physical problem, which is often unknown, $\hat{f}$ be the solution of the finite element model, and ε_d be the discretization error. The following equation can then be written:

$$f_{\text{true}} = \hat{f}(x, h) + \varepsilon_d(x, h) \tag{1}$$

where x is the input vector, and h is the mesh size (a smaller value of h is assumed to represent a finer mesh). The analysis is assumed to be conducted at a given input; therefore, the input x is dropped henceforth. The finer the mesh, the closer $\hat{f}$ is expected to be to f_{true}. The discretization error is assumed to be a polynomial function in mesh size, written as a series expansion,

$$f_{\text{true}} = \hat{f} + g_1 h + g_2 h^2 + \ldots \tag{2}$$

where $g_1, g_2, \ldots$ are functions that do not depend on discretization. Generalized Richardson extrapolation estimates true solution f_{true} by assuming a pth-order convergence in the series expansion. In the asymptotic range for sufficiently small mesh sizes, the leading error term shown next dominates the series expansion, and the preceding expression can be written as

$$f_{\text{true}} = \hat{f} + Ah^p \tag{3}$$

where A is a constant to be determined. To determine the unknown values of f_{true}, A, and p, the finite element mesh is solved at three mesh sizes h_1, h_2, and h_3. Mesh doubling or halving, although not necessary, is commonly done to simplify the equations. For a

Received 19 November 2010; revision received 1 March 2011; accepted for publication 15 March 2011.

*Research Associate, Department of Civil and Environmental Engineering.
†Ph.D. Student, Department of Civil and Environmental Engineering.
‡Professor, Department of Civil and Environmental Engineering; sankaran.mahadevan@vanderbilt.edu (Corresponding Author).

constant mesh refinement ratio, $r = h_3/h_2 = h_2/h_1$, the order of convergence p can be written as

$$p = \frac{\log[(f_3 - f_1)/(f_2 - f_1)]}{\log r} \tag{4}$$

The value of f_{true} is given as

$$f_{\text{true}} \approx f_1 - \frac{f_2 - f_1}{r^p - 1} \tag{5}$$

Several enhancements to the basic Richardson extrapolation technique described previously have been proposed in the literature. Richards [12] extended Richardson's extrapolation theory to include time and space discretization for time-dependent problems. Roache [5] (p. 125) and Marchi and Silva [13] consider multidimensional problems where mesh refinement is possible in more than one direction. Roache [5] further proposed the notion of grid convergence index to facilitate uniform and consistent reporting of grid convergence studies by multiple authors. The concept approximately relates the results from any grid convergence test to those expected from grid doubling of a second-order method. Soroushian et al. [14] discuss the errors associated with the Richardson extrapolation and estimate an asymptotic upper bound for the errors.

Some criticisms of the polynomial model in the Richardson extrapolation exist in the literature. The assumption of small mesh sizes and the requirement to be in the asymptotic range are often difficult to ensure. Rational functions [15–17] have been considered as an alternative to the polynomial model assumed in Eq. (3) [18,19]. Kammer et al. [20] used rational functions in Richardson extrapolation to build a response surface that includes the effects of discretization error on uncertainty quantification. We will discuss rational functions in more detail later in the paper. Computational fluid dynamics (CFD) codes are often known to exhibit oscillatory convergence patterns as the mesh size is reduced; Celik et al. [21] consider alternate representations of the error function using sinusoidal functions.

Because of the preceding reasons, caution is to be exercised when Richardson extrapolation is employed for error estimation. However, when using commercial finite element codes such as ANSYS [22], users often may have limited access to the source code of the solver to implement energy norm-based global error estimation techniques. Moreover, such techniques are more useful for adaptive mesh refinement than quantification of actual error. Oftentimes, in commercial codes, such error estimation options may be available only in one disciplinary solvers but not in the others. For example, to the best of our knowledge, ANSYS supports discretization error estimation for only some disciplinary solvers (e.g., structure solver) but not others (e.g., fluid solver). Error information from a single discipline may not be of great value when the focus is on coupled MDA. For the preceding reasons, we adopt the basic concept of Richardson extrapolation in this paper, but we propose several significant improvements to enhance its accuracy for MDA.

Numerical solution errors in multidisciplinary problems are largely dependent on the solution approach used to enforce compatibility among the disciplines. Several methods are used to solve MDA problems [23,24], e.g., the monolithic method (also known as the tightly coupled approach) and the partitioned method (also known as the staggered or loosely coupled approach). In monolithic methods, the entire MDA is treated as a monolithic entity or a single computational domain, and all the analyses are advanced simultaneously in time. While this approach can ensure conservation of properties and improved accuracy, it requires high computational time. Moreover, disciplinary analyses typically have distinct mathematical properties and software platforms, and a monolithic approach may be difficult to implement.

Partitioned methods, on the other hand, are loosely coupled. The disciplinary analyses are carried out separately in a sequential manner until the iterations converge. The interaction among disciplines is accounted for by data exchange (boundary conditions) along the interface of the disciplines. The advantage of such a staggered scheme is its modularity; it can be easily implemented into well-established disciplinary solvers. However, accuracy and stability are of concern, especially when the disciplinary meshes are nonconforming; that is, the nodes of the disciplinary meshes do not match at the interface [25]. There exists extensive literature in the area of nonconforming mesh interfaces within the context of FSI [26–30]. It is generally agreed that partitioned solution schemes cannot always guarantee conservation of properties. The relationships between conservation, stability, and accuracy for monolithic and partitioned methods are studied in [24].

Within the context of multidisciplinary design optimization, various solution architectures are used to enforce feasibility among the multiple disciplines [31–35]. Five major approaches are available in the literature: multidisciplinary feasible (MDF), individual discipline feasible (IDF), simultaneous analysis and design (SAND), collaborative optimization (CO), and concurrent subspace optimization (CSSO). The MDF method enforces multidisciplinary compatibility at each iteration of the optimization, while the IDF approach enforces only disciplinary feasibility at each iteration. The SAND approach includes disciplinary constraints as equality constraints within the formulation. CO and CSSO are multilevel formulations where the individual disciplines generally run suboptimizations and satisfy disciplinary compatibility while a system-level optimizer enforces multidisciplinary compatibility.

In the current paper, we are interested in discretization error quantification in the system output of coupled multidisciplinary analyses. While most existing work studies the impact of disciplinary meshes and their mismatches, the focus has been primarily on the disciplinary outputs/inputs. For example, [30] studies the effect of mesh mismatch on the errors in the load vector being exchanged between the fluid and structure disciplines. There is little to no work in the literature that considers the effect of discretization on the system output (this issue is discussed later in Sec. II), e.g., the lift value, which is obtained after the iterations of the fluid and structure analyses have converged. In FSI problems, Farhat et al. [36] provide guidelines for orders of global discretization error for the converged system-level output as a function of the individual fluid and structure errors. These guidelines are perhaps applicable only to the specific application of FSI, which may not be generally applicable to multidisciplinary analyses involving other disciplines, such as thermal-structure and thermal-fluid analyses.

While Richardson extrapolation has been used for problems that require multidimensional mesh refinement, its use for MDA problems has not been explored. The distinguishing feature of MDA problems in comparison with the existing Richardson extrapolation applications is that there are, typically, multiple disciplinary meshes involved. Moreover, mismatched disciplinary meshes at the interface contribute additionally to the discretization error in the system output, and there are no easy yet quantitative methods that can be implemented using existing commercial solvers.

In this paper, we adopt the Richardson extrapolation technique because of its ease of use and implementation, and we extend the theory to consider meshes of different disciplines, each with multidimensional mesh refinement, as well as interface mesh mismatch effects. Two alternative error representations for the multidisciplinary system are presented: 1) ignoring the mesh mismatch at the interface (Sec. III) and 2) including the mesh mismatch at the interface (Sec. IV). The error models in the second case are generally more complex than those in the first case. The error models in the first case are assumed to be functions of the disciplinary mesh refinements alone, whereas the error models in the second case have additional mesh mismatch variables.

For the simpler case of matching interfaces, we employ polynomial and rational function models for the error function. As mentioned previously, a rational function model is known to overcome some of the drawbacks of the traditional polynomial-based Richardson extrapolation. Consideration of mesh mismatch requires more variables and dimensions, and the well-known drawbacks of a polynomial error model can become more predominant. Therefore, for the second case including mesh mismatch, we investigate rational function and Gaussian process (GP) models for the error function. The GP model [37] provides a probabilistic framework for learning

the underlying error model, which can then be used to estimate the true function value.

Using polynomial/rational function models to represent discretization error is consistent with the existing practice in the literature, which involves making assumptions about the characteristics of the underlying error function. However, there can be some ambiguity involved, since the functional form of the error model, which is consistent with the data (mesh tests), is not unique. Rational functions are known for their flexibility to fit a data set; however, the accuracy of their predictions cannot be readily estimated (discussed later in Sec. V.A).

By proposing the use of a GP model, we focus on learning the underlying relationship between the data (mesh tests) and the true function value, which can only be observed empirically. Since Gaussian processes do not require explicit specification of a functional form, the issue of choice of the model form for the error function is resolved. Prediction using GP models has been in practice for a long time [37] and, in this paper, we adopt this popular tool within the context of discretization error estimation.

As the system mesh tests for MDA are computationally expensive to perform, it is desirable that the estimation of the underlying error model be based on a small number of mesh tests. Moreover, it is not usually feasible to conduct mesh tests close to the desired prediction location, since it requires infinitesimally small mesh sizes. In this context, a GP model offers significant advantages over polynomial and rational function models, as discussed in Sec. V.A.

The proposed error models are illustrated using a 3-D FSI problem (Sec. VI) for an aircraft wing, which is analyzed using the commercial solver ANSYS.

II. Multidisciplinary Analysis Preliminaries

In this section, we present the notation and mathematical definitions of the MDA problem used in this paper.

For simplicity of presentation, two disciplines are considered, A_1 and A_2, with feedback coupling, as shown in Fig. 1. The outputs of discipline A_1 are inputs to discipline A_2 and vice versa. Let x_{A1} and x_{A2} be the vectors of inputs to the individual disciplines A_1 and A_2, respectively, and let x_s be the vector of shared inputs. Let $\hat{y}$ be the system-level output, the quantity for which the discretization error is to be estimated. Let h_{A1_x}, h_{A1_y}, and h_{A1_z}, respectively, be the mesh sizes in the X, Y, and Z directions for A_1, and let h_{A2_x}, h_{A2_y}, and h_{A2_z}, respectively, be the mesh sizes in the X, Y, and Z directions for A_2. The quantities u and v denote the disciplinary outputs/inputs being exchanged. The following presented discussion can also be extended to multidisciplinary analyses with more than two disciplines. A similar form of the error functions as presented in the next section can be assumed for problems with two or more disciplines.

In this paper, we approach the discretization error estimation problem from the perspective of the system output $\hat{y}$, because that is the quantity of interest in MDA. Instead of considering the discretization errors in the outputs/inputs (u and v) of individual disciplines, we focus on $\hat{y}$, because the functional relationship between the disciplinary discretization errors and the system discretization error is not exactly known. Moreover, estimation of disciplinary discretization errors typically requires mesh tests at the disciplinary level. The disciplinary outputs before the final convergence of $\hat{y}$ do not always satisfy interdisciplinary compatibility. Therefore, we believe that mesh tests of the entire system are more informative than disciplinary mesh tests.

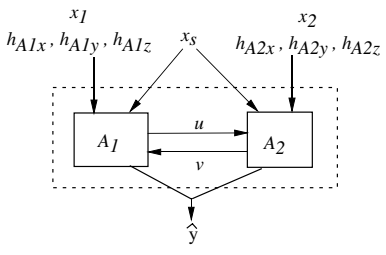

Fig. 1 Illustration of multidisciplinary system with feedback.

Another pertinent issue of discussion regarding errors in MDA is the type of coupling among the subsystems. In feedforward MDA, there is unidirectional coupling among disciplines. The contribution of the mesh mismatch to the system discretization happens only once. In feedback systems, however, there is bidirectional coupling among disciplines. At each fixed-point iteration of the system analysis, the interface contributes twice to system discretization error (e.g., once from fluid to structure, and back from structure to fluid). In a staggered solution implementation, if the system analysis takes 10 or 20 iterations to converge, the discretization error in the disciplinary inputs/outputs (e.g., pressure values and displacement values) builds up. The approximations made during the exchange of boundary conditions not only impact the discretization error of the output solution but also the conservation of quantities across the interface, thereby affecting the accuracy of the solution. In this paper, we focus on the system output discretization error alone.

III. Proposed Discretization Error Models: No Mesh Mismatch

In this section, we discuss the details of the proposed discretization error models without consideration of mesh mismatch. We present two discretization error models that assume that the meshes match topologically at the interface. The error models in this case are assumed to consist of only the disciplinary mesh refinement variables; the discretization error in $\hat{y}$ can predominantly be considered a function of the six mesh sizes shown in Fig. 1.

A. Polynomial Function Error Model: No Mesh Mismatch

The polynomial error model discussed here is an extension of the generalized Richardson extrapolation presented in Sec. I. For the MDA problem described in Sec. II, the system output $\hat{y}$ (Fig. 1) of the computational model and y_{true} are related as

$$y_{\text{true}} = \hat{y}(x_{A1}, x_{A2}, x_s, h_{A1_x}, h_{A1_y}, h_{A1_z}, h_{A2_x}, h_{A2_y}, h_{A2_z}) + \varepsilon_d(x_{A1}, x_{A2}, x_s, h_{A1_x}, h_{A1_y}, h_{A1_z}, h_{A2_x}, h_{A2_y}, h_{A2_z}) \tag{6}$$

where ε_d is the discretization error in the system output $\hat{y}$. We assume that the analysis is conducted for a given x_{A1}, x_{A2}, and x_s, so these quantities are dropped in equations henceforth. A power series expansion for ε_d in the preceding expression provides the following equation:

$$\varepsilon_{d_{P1}} = \{m_1(h_{A1_x}) + \ldots + m_6(h_{A2_z})\} + \{m_k(h_{A1_x}h_{A1_y}) + \ldots + m_n(h_{A2_y}h_{A2_z})\} + \{m_{n+1}(h_{A1_x})^2 + \ldots + m_{n+7}(h_{A2_z})^2\} + \ldots, \text{HOT} \tag{7}$$

where m_i, $i = \{1, \ldots, n+7\}$ is the corresponding coefficient, HOT denotes higher-order terms. In the proposed polynomial model, it is assumed that each mesh refinement parameter potentially has a different order of convergence. For example, increasing the number of structural elements in the lateral direction of an aircraft wing model can impact the solution error differently when compared with increasing the number of fluid elements in the direction of fluid flow.

Assume that each mesh refinement parameter has its own asymptotic order of convergence; the term associated with this order is assumed the dominant contributor to the discretization error, and the remaining terms are neglected. The following simplified estimate of the discretization error is obtained:

$$\varepsilon_{d_{P1}} = B_1(h_{A1_x})^{p_{A1_x}} + B_2(h_{A1_y})^{p_{A1_y}} + B_3(h_{A1_z})^{p_{A1_z}} + B_4(h_{A2_x})^{p_{A2_x}} + B_5(h_{A2_y})^{p_{A2_y}} + B_6(h_{A2_z})^{p_{A2_z}} \tag{8}$$

where B_i, $i = \{1, \ldots, 6\}$ is the coefficient for the ith mesh refinement parameter, and $p_{A_{j_k}}$ is the order of convergence for the jth disciplinary mesh in the kth direction. Using the preceding equation for multidisciplinary multidimensional Richardson extrapolation,

there are a total of 13 unknown quantities: six orders of convergence, six coefficients, and the true solution. This requires 13 mesh tests to determine the unknown quantities. Depending on the specific problem at hand (e.g., symmetry conditions), some of the preceding coefficients may be assumed to be equal (e.g., $p_{A1_y} = p_{A1_x}$) to reduce the number of unknowns.

A drawback of the preceding approach is that the error model assumed does not consider any cross effects of the mesh size parameters. Moreover, as discussed previously, the assumption of asymptotic convergence is much more difficult to verify in multiple dimensions. Also, note that 13 simulations are needed to compute an estimate of discretization error, even without explicitly accounting for interaction terms. Therefore, in the next subsection, a rational function model for the discretization error is presented. As discussed in Sec. I, a rational function approximation is considered a better alternative to the polynomial model for Richardson extrapolation.

B. Rational Function Error Model: No Mismatch

Rational functions are generally capable of reproducing data with fewer coefficients than those required for a polynomial representation [38]. A rational function is the ratio of two polynomials; while there are several forms of rational functions, the following is considered in this paper:

$$F(x) = \frac{P(x)}{Q(x)} = \frac{a_0 + a_1 x + \ldots, a_m x^m}{b_0 + b_1 x + \ldots, b_n x_n} \tag{9}$$

where $Q(x) \neq 0$. The preceding equation represents a rational function of the order (m, n). By convention, the lead constant term in the denominator b_0 is assumed to be 1. Then, the rational polynomial of the order (m, n) requires $m + n + 1$ coefficients to be estimated. Although rational functions can be of any order, those that assume $m = n$ or $m = n + 1$ tend to minimize the number of coefficients to be estimated [38].

For multiple variables, a rational function can be represented as follows:

$$F(\hat{\mathbf{x}}) = \frac{P(\hat{\mathbf{x}})}{Q(\hat{\mathbf{x}})} = \frac{\sum_{j=0}^{J} c_j p_j(\hat{\mathbf{x}})}{\sum_{k=J+1}^{R} c_k q_k(\hat{\mathbf{x}})} \tag{10}$$

where $\hat{\mathbf{x}}$ is the vector of independent variables; p_j and q_k are functions of independent variables; and $\mathbf{c}$ is the vector of unknown coefficients that must be estimated.

For a rational function error model, again consider Eq. (6), which is repeated:

$$\begin{aligned} y_{\text{true}} &= \hat{y}(h_{A1_x}, h_{A1_y}, h_{A1_z}, h_{A2_x}, h_{A2_y}, h_{A2_z}) \\ &\quad + \varepsilon_d(h_{A1_x}, h_{A1_y}, h_{A1_z}, h_{A2_x}, h_{A2_y}, h_{A2_z}) \end{aligned} \tag{11}$$

A generic rational function representation of $\varepsilon_{d_{R1}}$ can be written as

$$\begin{aligned} &\varepsilon_{d_{R1}}(h_{A1_x}, h_{A1_y}, h_{A1_z}, h_{A2_x}, h_{A2_y}, h_{A2_z}) \\ &= \frac{d_0 + \{\mathbf{d}_1[h_{A1_x}, \ldots, h_{A2_z}]^T\} + \{\mathbf{d}_2[h_{A1_x}h_{A1_y}, \ldots, h_{A2_y}h_{A2_z}]^T\} + \{\mathbf{d}_3[h^2_{A1_x}, \ldots, h^2_{A2_z}]^T\} + \text{HOT to } m\text{th power}}{1 + \{\mathbf{t}_1[h_{A1_x}, \ldots, h_{A2_z}]^T\} + \{\mathbf{t}_2[h_{A1_x}h_{A1_y}, \ldots, h_{A2_y}h_{A2_z}]^T\} + \{\mathbf{t}_3[h^2_{A1_x}, \ldots, h^2_{A2_z}]^T\} + \text{HOT to } n\text{th power}} \end{aligned} \tag{12}$$

where $\mathbf{d}_1$, $\mathbf{d}_2$, and $\mathbf{d}_3$ are row vectors of coefficients of the linear terms, cross terms, and quadratic terms of the numerator, respectively, and $\mathbf{t}_1$, $\mathbf{t}_2$, and $\mathbf{t}_3$ are those for the denominator, respectively. Choosing the exact form of a rational function can involve some trial and error, depending on the nature of the problem. One specific guideline that can be followed for the choice of the rational function form for discretization error is that the error is generally expected to decrease as the mesh becomes finer in all dimensions and all disciplines. Note that the preceding rational function form of $\varepsilon_{d_{R1}}$ includes interaction terms of the form $h_{A1_x}h_{A1_y}$, unlike the polynomial model shown previously. Once the specific form of a rational function for a given problem is chosen, the number of mesh tests that must be performed is $M + 1$, where M is the total number of unknown coefficients to estimate the unknown true solution.

In the error models discussed so far, we assumed that the disciplinary meshes match at the interface. In the more realistic case of mismatched meshes, the discretization error of the converged solution also depends on the extent of mesh mismatch. Additional complexities arise for mismatched meshes in terms of imposing governing equations as boundary conditions, conservation of properties, and accuracy. As discussed previously, MDA analysis can be conducted either using a monolithic or staggered approach. In this paper, we focus on the staggered approach in particular, where the effects of interface mismatch can be significant.

IV. Proposed Discretization Error Models: With Interface Mesh Mismatch

In staggered solution approaches, information is typically transferred at the boundaries; for example, pressures and displacement boundary conditions are exchanged at the wet surface of a wing for the FSI problem. In most practical problems, the meshes at the interfaces do not match with each other, as shown in Fig. 2. This commonly happens because disciplinary meshes may be built using different solvers. Moreover, a finer mesh may be required for one of the disciplinary meshes to obtain convergence; for example, fluid meshes typically require finer meshes to capture boundary-layer effects. Because of the lack of one-to-one correspondence of nodes at which information is exchanged, approximations must be made in the data exchange.

For example, consider the boundary conditions being sent from disciplinary mesh 1 to mesh 2 in Fig. 2. The nodes sending information (solid circles) do not match topologically with the nodes receiving information (open circles); there is a mismatch at points **A** and **B** on the receiving mesh and points **C** and **D** on the sending mesh. For such mismatched meshes at the interface, some approximations, such as interpolations, have to be made to transfer boundary conditions, thereby causing an error in the disciplinary inputs/outputs. This error can be formulated in terms of the orders of the interpolating functions on the sending/receiving meshes [28]. The amount of this error depends on the mesh refinement in the two meshes and the extent of mismatch. Thus, this error contributes to the overall discretization error of the system output.

There are several load transfer schemes (such as node projection, quadrature projection, and common refinement schemes) available in the literature that study this issue in more detail [29,30,36,39]. Some researchers have developed a metric that quantifies grid mismatch [30] and assesses the impact of mesh mismatch on the preceding three load transfer schemes in fluid–structure problems. They study errors in the solutions at the interface and the disciplinary solutions. In this paper, we are interested in the discretization error in the system output of the MDA (e.g., lift or drag) as against those in pressures or displacements being exchanged at the interface.

In the next subsection, we explicitly consider the effects of disciplinary mesh sizes, as well as the interface mesh mismatch on the system discretization error. We first define a metric to characterize mesh mismatch at the interface along each spatial direction. As

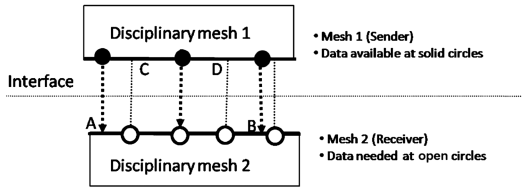

Fig. 2 Nonconforming meshes at interface.

mentioned previously, some metrics exist in the literature that quantify mesh mismatch [30]. We denote the mesh mismatch along each spatial direction as mm_x, mm_y, and mm_z, respectively; a higher value of this metric is assumed to indicate a stronger mismatch when compared with a lower value.

In the example presented later in the paper, and for the mesh refinement scheme considered, we simply use the difference between mesh sizes as an indicator of mesh mismatch along each direction. We parenthetically note that mm_x, mm_y, and mm_z are not independent variables, since they are derived from the mesh refinement parameters. It can be argued that these mesh mismatch variables, which cannot be explicitly designed in a set of mesh experiments, need not be explicitly considered in the error model. We, however, consider the mesh mismatch variables in the error model, since these are of particular interest in MDA discretization error estimation.

Using the terminology defined in the earlier sections, we write the following equation for system discretization error for MDA, where the discretization error is a function of the disciplinary mesh sizes and the mismatches along the three spatial directions:

$$f_{\text{true}} = \hat{f} + \varepsilon_d(h_{A1_x}, h_{A1_y}, h_{A1_z}, h_{A2_x}, h_{A2_y}, h_{A2_z}, mm_x, mm_y, mm_z) \tag{13}$$

Note that, in the literature, the error function was assumed to be a power series expansion in terms of the mesh size. As discussed in Sec. I, assuring that the asymptotic convergence assumption holds is a challenge even for single dimensional mesh refinement. The assumption of asymptotic convergence is much more difficult to verify in multiple dimensions with several disciplinary meshes that are not matching. Moreover, such a polynomial model does not consider any cross effects of the mesh size parameters. Therefore, we use rational function and GP models for the error functions with mesh mismatch.

We make the following observations on how the mesh size and mismatch can generally affect the discretization error:

1) We assume, as is generally expected, that as the mesh is refined in all dimensions, the solution is closer to the true solution (exceptions have been noted in the literature as pointed out in Sec. I).

2) If the meshes match topologically at the interface, we assume that the interface contribution to the discretization error can be neglected.

3) We extrapolate the proposed error models to the point where all the mesh refinement variables tend to zero and where the meshes match at the interface.

A. Rational Function Error Model: With Mesh Mismatch

To account for the two primary effects of interest (namely, disciplinary mesh refinement and interface mesh mismatch), a few assumptions are made. While alternate representations are possible, we define the following two variables for simplicity. Let $h_d = f_d(h_{A1_x}, h_{A1_y}, h_{A1_z}, h_{A2_x}, h_{A2_y}, h_{A2_z})$ and $h_{mm} = f_{mm}(mm_x, mm_y, mm_z)$. Formulating the error function in terms of a reduced set (h_d and h_{mm}) instead of the complete set minimizes the number of variables in the rational function, thereby decreasing the number of unknown coefficients to be estimated using expensive mesh tests. For example, f_d and f_{mm} can be assumed to be a weighted sum of the corresponding mesh variables, where the weights can be used to account for element sizes of largely different magnitudes. Alternate formulations for f_d and f_{mm} include using products of the corresponding mesh variables. It should be noted that f_{true} can be sensitive to the form of f_d and f_{mm} chosen. In cases where multidisciplinary mesh tests are computationally more affordable, use of h_d and h_{mm} can be avoided to reduce this sensitivity to the functional form. Moreover, fewer variables/coefficients can restrict the flexibility of the fit of the rational function, and they can affect the true predicted value. We propose a rational function representation of ε_d in terms of h_d and h_{mm} as

$$\varepsilon_{d_{R2}}(h_d, h_{mm}) = \frac{c_1 + c_2 h_d + c_3 h_{mm} + c_4 h_d h_{mm} + c_5(h_d^2 + h_{mm}^2)}{1 + c_2 h_d + c_3 h_{mm}} \tag{14}$$

where $c_1, \ldots, c_5$ are unknown coefficients to be estimated. While there may exist other valid forms, we use the assumptions noted at the end of the previous subsection to use the preceding specific form. Note that this form of $\varepsilon_{d_{R2}}$ includes interaction terms of the form $h_d h_{mm}$, which is expected to model the cross effects between the contributions of disciplinary mesh refinement and interface mismatch effects.

As discussed in Sec. I, the true function value, as extrapolated using such parametric models, strongly depends on the functional form being assumed, and there is large subjectivity involved in this choice. In the next subsection, we discuss the use of Gaussian processes, which do not require explicit specification of a functional form.

B. Gaussian Process Error Model: With Mesh Mismatch

GP surrogate models have been widely used in a range of applications, particularly in regression and prediction [37]. The GP is a generalization of the multivariate Gaussian distribution and can be viewed as a collection (indexed by points in the domain) of multivariate Gaussian random variables. Unlike the polynomial and rational function models that model the underlying functional form directly, a GP instead models the covariance between the training data using a Bayesian inference methodology. Training data refer to set of mesh refinement combinations and the corresponding values of $\hat{y}$:

Let $\hat{f}$: $\boldsymbol{\Omega} \to \Re$, $\boldsymbol{\Omega} \in \Re^{\mathbf{D}}$ be the underlying function that we are interested in learning. The set $\boldsymbol{x}_T = \{\boldsymbol{x}_1, \boldsymbol{x}_2, \ldots, \boldsymbol{x}_t | \boldsymbol{x}_i \in \Omega\}$ represents the t training points or the mesh tests, where

$$\boldsymbol{x}_i = \{h_{A1_x}, h_{A1_y}, h_{A1_z}, h_{A2_x}, h_{A2_y}, h_{A2_z}, mm_x, mm_y, mm_z\}^T$$

The set $\mathcal{D}_T = \{\boldsymbol{x}_T, \boldsymbol{y}_T\}$ represents the training data, where $\boldsymbol{y}_T = \{\boldsymbol{y}_1, \boldsymbol{y}_2, \ldots, \boldsymbol{y}_t | \boldsymbol{y}_i = f(\boldsymbol{x}_i) + \epsilon_i\}$ is the set of measured function values or samples, $\epsilon_i \sim \mathcal{N}(0, \sigma_n^2)$ is the measurement noise, and $\boldsymbol{f}_T = \{\hat{f}_1, \hat{f}_2, \ldots, \hat{f}_t\}$ is the set of the system outputs at each mesh configuration.

The objective is to generalize the information contained in the data $\mathcal{D}_T$ so as to infer the value of the underlying function $\boldsymbol{f}_P$ at any arbitrary set of p prediction points $\boldsymbol{x}_P \in \Omega$. A GP is defined by a mean function $m(\boldsymbol{x})$ and the covariance function $k(\boldsymbol{x}, \boldsymbol{x}')$. In general, these functions must be selected so as to reflect our assumptions about the underlying function, such as about its stationarity, periodicity, etc. [37]. As is common in literature [37], in this paper, it is assumed that the mean function, $m(\cdot) = 0$, and the covariance function are the squared exponential function,

$$k(\boldsymbol{x}_i, \boldsymbol{x}_j; \theta) = \theta_1 \exp\left[-\frac{1}{2}\sum_{d=1}^{D}\frac{(x_i - x_j)^2}{l_i}\right] \tag{15}$$

Together, $\boldsymbol{\Theta} = \{\mathbf{l}, \theta_1, \sigma_n\}$ form the parameters of the covariance function, and thus of the GP model. These parameters must be inferred from the given data to make predictions. A common method employed is the maximization of the log marginal likelihood [37]. Of special interest are the parameters, $\mathbf{l} = \{l_1, l_2, \cdots, l_D\}$, known as the length scale parameters, which correspond to the length of the variation in function values implied by $k(\cdot)$ in each dimension of $\boldsymbol{\Omega}$. While a small value of l_i indicates a significant variation in the function values in the ith dimension, a large value of l_i indicates that

the variability in the function value is not impacted by changes in the ith dimension.

The GP model prediction is given by $p(\boldsymbol{f}_P|\boldsymbol{y}_T, \boldsymbol{x}_T, \boldsymbol{x}_P, \boldsymbol{\Theta}) \sim \mathcal{N}(\boldsymbol{m}, \boldsymbol{S})$, with

$$\boldsymbol{m} = \boldsymbol{K}_{PT}(\boldsymbol{K}_{TT} + \sigma_n^2 \boldsymbol{I})^{-1}\boldsymbol{y}_T \tag{16}$$

$$\boldsymbol{S} = \boldsymbol{K}_{PP} - \boldsymbol{K}_{PT}(\boldsymbol{K}_{TT} + \sigma_n^2 \boldsymbol{I})^{-1}\boldsymbol{K}_{TP} \tag{17}$$

where $\boldsymbol{K}_{TT} = [k(x_i, x_j)]_{i,j}$ is the $t \times t$ matrix of the covariances between the training points $\mathbf{X}_T$, $\boldsymbol{K}_{PP}$ is the $p \times p$ matrix of the covariances between the prediction points $\mathbf{X}_P$, and $\boldsymbol{K}_{PT}$ is the $p \times t$ matrix of covariances between $\mathbf{X}_P$ and $\mathbf{X}_T$ with $\boldsymbol{K}_{TP}$ as its transpose [37].

The mean $\boldsymbol{m}$ is taken to be the predicted value of the underlying function at the $\boldsymbol{x}_P$. This estimate is a function of the 1) measurement uncertainty, 2) the distances among the training points, 3) the measured values of the underlying function at the training points, and 4) the distances between the training points and the prediction points. By collecting all the terms that do not depend on the prediction points $\boldsymbol{x}_P$, Eq. (16) may be rewritten as

$$\boldsymbol{m} = \boldsymbol{K}_{PT}\boldsymbol{w}_T \tag{18}$$

where $\boldsymbol{w}_T = (\boldsymbol{K}_{TT} + \sigma_n^2 \boldsymbol{I})^{-1}\boldsymbol{y}_P$. The function value predicted by the GP model at a prediction location is thus a weighted sum of the correlation between the prediction location and each of the training points.

If a computer code is used to evaluate $\boldsymbol{f}_T$ or $\boldsymbol{y}_T$, typically, there is no measurement noise and σ_n may be set to zero. Under such circumstances, the GP regression model is interpolative, i.e., $m(\boldsymbol{x}_T) = \boldsymbol{f}_T$ and $S(\boldsymbol{x}_T) = 0$. However, in this paper, σ_n value is set to a very small value, so as to stabilize the inversion of the covariance matrix without affecting the value of the prediction numerically.

In the case of our current problem, we are interested in a single prediction point where the mesh sizes for all disciplines and dimensions are close to zero and the disciplinary meshes match with each other. In other words, once we train the GP model using mesh tests, we find the true value of the MDA output by predicting the function value at

$$\{h_{A1_x}, h_{A1_y}, h_{A1_z}, h_{A2_x}, h_{A2_y}, h_{A2_z}, mm_x, mm_y, mm_z\} = \{0, 0, 0, 0, 0, 0, 0, 0, 0\}$$

As discussed previously, GP models not only provide a mean prediction value of the true solution but also a prediction variance of the true value of the system output. However, the discretization error is a deterministic quantity, since it is a result of a computer simulation. The prediction variance associated with the true value of the system output can be interpreted from the perspective of mesh tests, discussed in the next section.

V. Mesh Tests and Fitting Error Models

Mesh tests are relatively easy to conduct when only a single mesh refinement possibility exists; mesh size doubling or halving is usually done in such cases. In the current paper, where we consider multidimensional and multidisciplinary mesh refinements, several combinations of directional and/or disciplinary mesh refinements are possible.

Two important factors in the goodness of the predictions of error models are the number of mesh tests and the combination of mesh refinements at which mesh tests are conducted. For different numbers and refinements, different values of the discretization error and the true function value are to be expected. Moreover, it is well known that multidisciplinary mesh tests are computationally expensive; it is therefore desirable to conduct as few mesh tests as possible. In this subsection, a brief discussion about mesh tests is provided: specifically, the questions of how many and what combinations are discussed.

A. Mesh Tests

The question of how many mesh tests are required has been typically answered by the number of unknown coefficients in the error model chosen, although it may be desirable to run as many mesh tests as feasible to get better estimates of the unknown coefficients. Functional forms with a higher number of unknown coefficients may offer more flexibility to fit the data. However, a higher number of unknowns may also require a higher number of mesh tests. We note that the rational and polynomial functions model the underlying functional form using these mesh tests, and we extrapolate this functional form to predict the true solution. GP models, on the other hand, model the covariance structure between the functional values, and they assume that the same covariance structure holds at the prediction point. This generally allows for a more accurate prediction of the true solution, even with fewer mesh tests.

As discussed previously, the GP model not only yields a mean value for the true function value but also a variance. As shown in Eq. (17), the variance of the GP prediction depends on the covariance among the prediction point (true value of the system output) and the mesh refinement combinations of the training data (where the mesh tests performed). This is an important advantage the GP model offers; we can quantitatively estimate the impact of the number of mesh tests on the true value of the function using the prediction variance. No such possibilities of assessing the impact of mesh tests on the true value readily exist for polynomial or rational function models.

The next question to be addressed is at what mesh refinement combinations the tests should be conducted, e.g., the particular values of $\{h_{A1_x}, h_{A1_y}, h_{A1_z}, h_{A2_x}, h_{A2_y}, h_{A2_z}\}$ at which the MDA should be conducted. As mentioned in Sec. I, for the simple case of a single discipline mesh with unidirectional mesh refinement, three mesh tests with an assumed grid refinement ratio are needed to determine the unknowns. For such problems, it is suggested in the literature that grid refinement ratios can be integers or nonintegers [5]. While it is relatively straightforward to refine or coarsen the mesh using a grid refinement ratio in a single dimension, the current problem involves six dimensions for mesh refinements in two disciplines, each of which can have a potentially different grid refinement ratio.

For illustration, consider Fig. 3. The dimensions of the cubes represent the grid refinement ratios in the corresponding directions, and each solid circle (black and gray) represents a particular combination of mesh refinement or coarsening when compared with the center of the cube. Note from Fig. 3 that many possibilities exist for refinement combinations at which mesh tests can be conducted. The specific choices for grid refinement out of these several possibilities can often be driven by the problem at hand, limitations of the software used to build and solve the computational model, and limitations of computational hardware. Once the mesh tests are conducted, the error models can be fit using the procedure discussed in the next subsection.

B. Fitting Error Models

The polynomial and rational function error models discussed so far require unknown parameters to be estimated by conducting mesh tests. Once an appropriate functional form of the error model is chosen, one possibility is to estimate the unknowns using a least-squares approach. Let $M + 1$ be the generic number of mesh tests conducted, resulting in a $\{1 \times (M + 1)\}$ vector of $\hat{\mathbf{y}}$. A least-squares optimization problem can be set up as follows to determine the unknown coefficients, given as

$$\min_{\mathbf{U}, y_{\text{true}}} \sum_{i=1}^{M+1} w_i \text{LS}_i \tag{19}$$

$$\text{where } \text{LS}_i = (y_{\text{true}} - \{\hat{\mathbf{y}}_i + \varepsilon_d\})^2 \tag{20}$$

where y_{true} is the true function value; w_i can be chosen as a normalizing factor; $\mathbf{U}$ is the vector of unknowns, which depends on the error model chosen; LS_i is the squared error corresponding to the ith mesh test, and ε_d depends on the error model chosen.

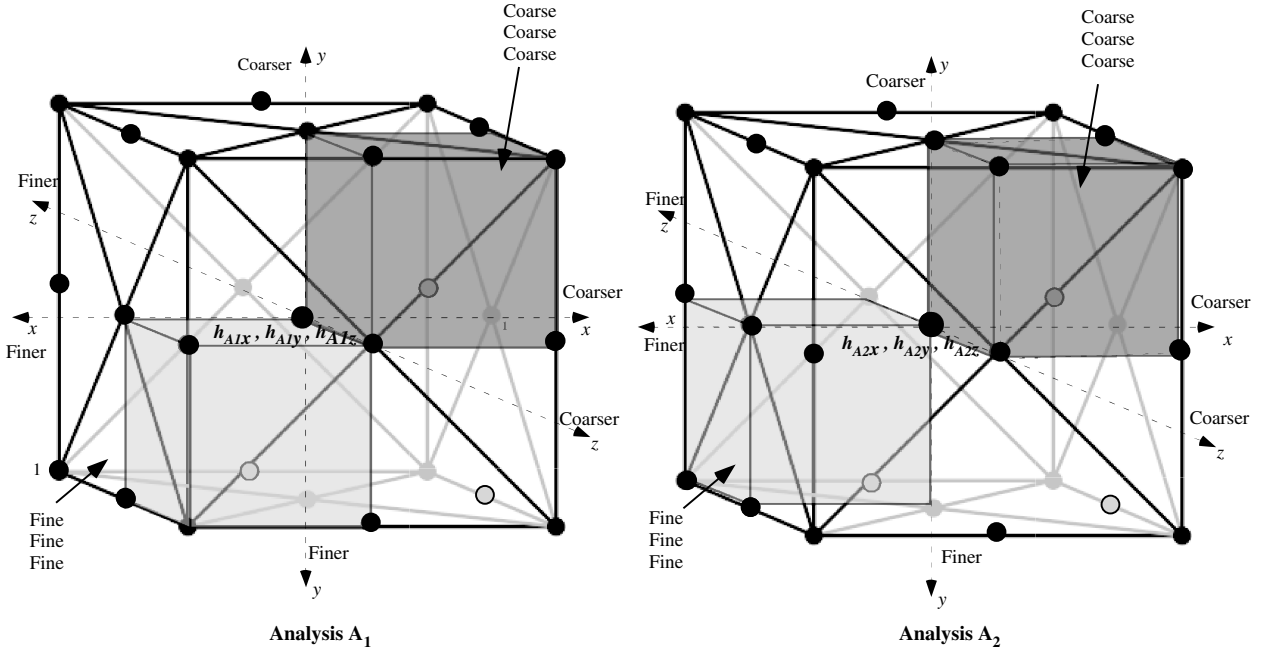

Fig. 3 Multidimensional mesh refinement for multiple disciplines (circles denote a particular mesh refinement combination for a discipline).

As discussed in Sec. IV.B, fitting GP models involves inferring $\boldsymbol{\Theta} = \{\mathbf{l}, \theta_1, \sigma_n\}$ from the data or mesh tests. In this paper, we adopt the maximization of the log marginal likelihood [37] to fit the GP model. A numerical example is presented next to illustrate the proposed discretization error estimation approaches.

VI. Numerical Example

A 3-D steady-state FSI problem is considered in this section. A cantilevered wing with a NACA 0012 airfoil is adopted from [40]; SI units are used in this paper. The solid wing is made of an isotropic material with a Young's modulus $E = 1.45 \times 10^{11}$ N/m^2 and a Poisson's ratio of 0.2. An angle of attack of 5 deg and a yaw of 0 deg are assumed. An altitude of 10,000 m with a freestream density of 0.4135 kg/m^3 and a freestream pressure of 2.65×10^4 N/m^2 are assumed with a freestream Mach number of 0.3. Figure 4 shows the top view of the wing configuration.

We are interested in finding the lift of the wing for a given backsweep angle, which is the angle made by line AD with the vertical in Fig. 4. The FEA and CFD models are built in the ANSYS environment using mapped meshing, which is considered a more accurate meshing approach for large 3-D problems [22]. An incompressible, turbulent flow model is used for the CFD analysis, and a nonlinear solver is used for the FEA analysis. The wing is modeled using 3-D SOLID45 elements [22], and fluid around the wing is modeled using 3-D FLUID142 elements [22]. The fluid boundary conditions include ambient pressure and velocity inlet conditions, and the include no-slip conditions on the wing. Clamped structural boundary conditions are used at the fixed end of the wing. The far-field boundary of the fluid analysis is considered at a distance of 15 times the average chord length from the bottom left corner of the wing. Figure 5 shows a schematic of the FSI problem being considered.

We implemented two alternate ANSYS models: one with matching nodes at the fluid–structure interface and the other with mesh mismatch.

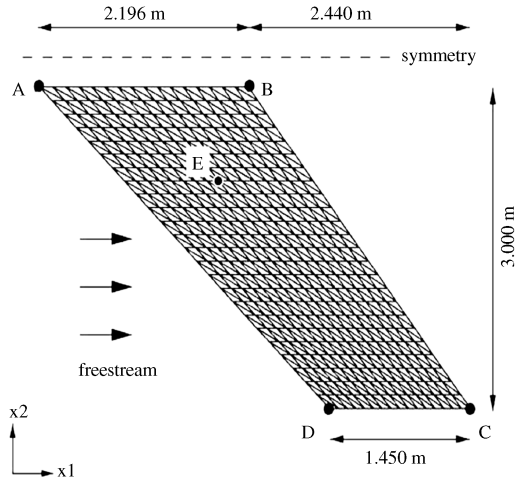

Fig. 4 Two-dimensional view of wing configuration (source: [40]).

A. Interface with Matching Meshes

Figure 6 shows the mesh configuration for the case of matching meshes at the interface. A staggering scheme is implemented to solve the MDA. ANSYS supports morphing of the fluid mesh to conform to the deformed structure mesh and transfer displacements to the structure mesh. Since there is one-to-one nodal correspondence for exchange of information in this case, we assume that the contribution of the interface to the discretization error is negligible. We ran this case for the finest mesh configuration possible within the limits of the academic version of the software, and we used it to benchmark the solution with the mismatched interface, since we do not know the true solution for this problem.

For the matched mesh case, a single parameter h_{ms} dictates the fineness of the mesh along the X and Y directions (cross section of the wing); h_{fm} and h_{wm}, respectively, control the fineness of the fluid mesh and structure mesh along the Z direction (length of the wing). These parameters (illustrated in Fig. 6) are the reciprocals of the number of divisions into which each line in a volume is divided; the

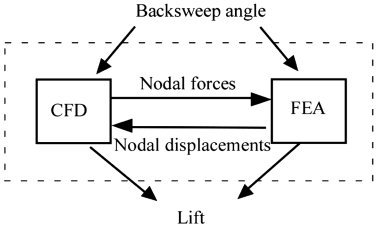

Fig. 5 FSI of wing problem.

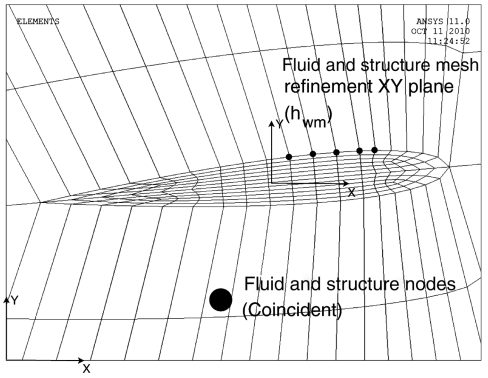

a) Front view of the wing and fluid meshes

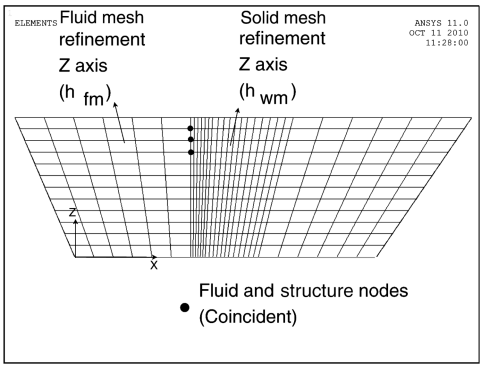

b) Top view of the wing and fluid meshes

Fig. 6 Matching fluid and structure meshes.

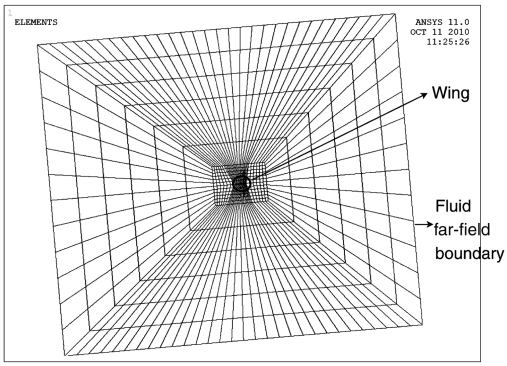

a) Overall view

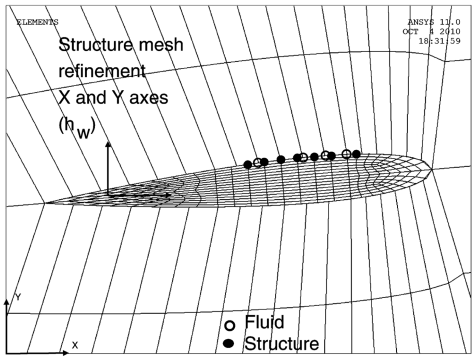

b) Fluid and Structure meshes: View 1

Fig. 7 Nonmatching fluid and structure meshes and refinement parameters.

smaller the values of these reciprocals, the higher the number of divisions, and hence finer the mesh. The polynomial error model for the no-mismatch case is shown:

$$\varepsilon_{d_{P1}} = A_{ms}(h_{ms})^{p_{ms}} + A_{fm}(h_{fm})^{p_{fm}} + A_{wm}(h_{wm})^{p_{wm}} \tag{21}$$

The preceding model has six unknown coefficients/exponents, in addition to the unknown $\text{lift}_{\text{true}}$ value. This implies that seven mesh tests are needed to compute the unknowns. The rational function error model that is used for this problem is

$$\varepsilon_{d_{R1}} = \frac{c_1 + c_2 h_{ms} + c_3 h_{fm} + c_4 h_{wm} + c_5(h_{ms}h_{fm} + h_{fm}h_{wm} + h_{wm}h_{ms}) + c_6(h_{ms}^2 + h_{fm}^2 + h_{wm}^2)}{1 + c_2 h_{ms} + c_3 h_{fm} + c_4 h_{wm}} \tag{22}$$

Note that the preceding expression is a simplified version of Eq. (12), with a quadratic polynomial in the numerator and a linear polynomial in the denominator. The coefficients in the rational function model are chosen so that the number of unknowns are the same for both polynomial and rational function models. The same seven mesh tests were used to compute the unknowns for both models, shown in Table 1.

Table 1 Mesh tests for parameter estimation: no mismatch

	$1/h_{ms}$	$1/h_{fm}$	$1/h_{wm}$	Lift force, N	Nodes
1	1	1	1	793.17	524
2	4	4	4	1,495.54	4,437
3	6	9	9	1,793.6	17,392
4	12	36	36	2,013.15	208,789
5	1	4	2	1,342.1	833
6	1	5	3	1,352.8	992
7	4	16	12	1,668.9	10,689

B. Interface with Mismatched Meshes

The multifield analysis module within ANSYS is used to implement mismatched mesh interfaces. ANSYS supports load transfer across interfaces with mismatched meshes; details are provided in [22]. The multifield solver continues to iterate until the quantities being exchanged converge or the maximum number of iterations are reached. To manage the computational expense, we imposed symmetries to reduce the number of possible mesh refinements to four, which are illustrated in Figs. 7 and 8. The parameters h_w and h_f dictate the mesh size along the X and Y directions for the structure (cross section of the wing) and fluid mesh, respectively; h_{zw} and h_{zf}, respectively, control the mesh size of the structure and fluid mesh, respectively, along the Z direction (length of the wing).

The relative mismatches along the X and Y directions for this example are assumed for illustration purposes to be $mm_x = mm_y = [(1/h_w) - (1/h_f)]$ and $mm_z = [(1/h_{zw}) - (1/h_{zf})]$. Accurately quantifying mesh mismatch for a 3-D problem is outside the scope of this paper. Note that the true predicted value can be sensitive to the form of mismatch chosen. Alternate forms for mismatch can be derived in terms of the maximum distance between a structural node and its nearest fluid node. As in Sec. IV, a mismatch variable is not an independent variable that can be designed in a mesh test, since it depends in some form on the mesh refinement combination chosen. To sufficiently capture the effect of mismatch on the true predicted value, it is desirable that the mismatch variables be adequately sampled. The form chosen in this paper, while simple, lends itself to uniform sampling of mismatch variables. While more accurate

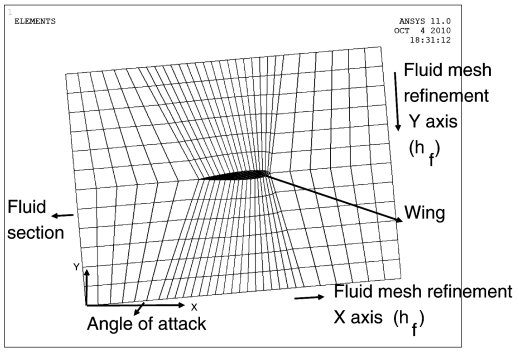

a) Fluid and structure meshes: view 2

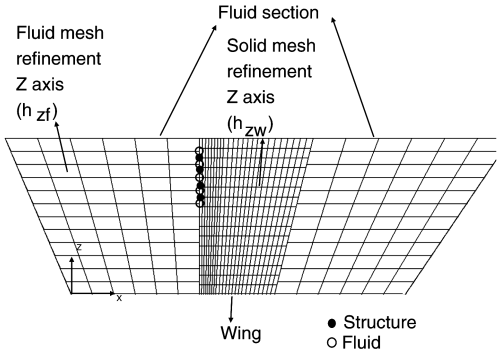

b) Fluid and structure meshes: view 3

Fig. 8 Nonmatching fluid and structure meshes and refinement parameters.

mismatch definitions are possible, they can pose sampling challenges, thereby not adequately capturing the mismatch aspects on the discretization error.

Because of the imposed symmetry, $mm_x = mm_y$; therefore, only mm_x is considered as a variable in the error model. A large value of mismatch variable indicates that there is a severe discrepancy in the relative mesh sizes of the fluid and the structure when compared with a lower value. Negative values of mm_x and mm_z indicate that the structure mesh is coarser than the fluid mesh.

Eight mesh tests with different mesh refinement combinations, shown in Table 2, were run for a zero backsweep angle. In problems with multidisciplinary and multidimensional mesh refinement, it is difficult to verify if the asymptotic convergence assumption is valid; the polynomial error model can yield inaccurate results for such cases. The mesh tests in the paper consider a wide range of mesh refinement combinations, where some element sizes are relatively coarse. Rational function and GP error models can be used over such a wide range, since they relax the requirement of asymptotic convergence.

To illustrate the impact of mesh refinement combinations on the predicted true value, we chose three sets of six mesh tests each (from Table 2), and error models were trained for each set. Set 1 consists of mesh refinement combinations in rows {1, 2, 3, 5, 6, 7}, set 2 consists of rows {2, 3, 4, 5, 6, 7}, and set 3 consists of rows {1, 3, 5, 6, 7, 8} in Table 2.

Table 2 Mesh tests with mismatch: set 1 rows {1, 2, 3, 5, 6, 7}, set 2 rows {2, 3, 4, 5, 6, 7}, and set 3 rows {1, 3, 5, 6, 7, 8}

	$1/h_w$	$1/h_f$	$1/h_{zw}$	$1/h_{zf}$	mm_x	mm_z	Lift, N	Nodes
1	14	14	12	10	0	2	1,940.3	183,182
2	14	14	14	12	0	2	2,011.5	218,048
3	16	12	10	10	4	0	1,850.5	130,880
4	10	12	14	12	−2	2	1,788.7	157,402
5	10	14	16	12	−4	4	2,011.5	211,730
6	12	14	14	14	−2	0	2,016.6	246,878
7	6	12	12	14	−6	−2	1,966.7	191,088
8	14	12	12	12	2	0	1,788.9	162,736

The rational function error model that is used for this example is shown in Eq. (14), where

$$h_d = f_d(h_w, h_f, h_{zw}, h_{zf}) = h_w + h_f + h_{zw} + h_{zf}$$

and

$$h_{mm} = f_{mm}(mm_x, mm_y) = mm_x \times mm_y$$

For the example in the paper, f_d is chosen simply as the sum of the element sizes, since the variables are of comparable magnitudes. For the example in the paper, we observed that a large discrepancy between element sizes results in large mismatches that pose convergence challenges in ANSYS. The form of f_{mm} was chosen as a product, since the mismatch variables can assume negative or positive values, and an additive form can misleadingly yield a zero value for h_{mm}.

Various mesh refinement combinations are considered (Table 2), e.g., coarse fluid mesh and fine structure mesh, and vice versa, low/high mesh mismatch in XY plane, low/high mesh mismatch along the Z axis, etc. The resources of the Advanced Computing Center for Research and Education at Vanderbilt University have been used to run the tests. Mesh test 1 (fewer nodes) in Table 1 requires about 0.36 s, and mesh test 6 (higher number of nodes) in Table 2 requires about 54 min. For sets 1, 2, and 3, the optimization formulation presented in Sec. V.B is solved to estimate the unknowns for the rational function model. To alleviate issues of local optima, global optimization tools from the TOMLAB suite of optimizers [41] are used. The results are summarized in Table 3.

As mentioned previously, the mean value given by the GP model is taken as the prediction [Eq. (16)], with the prediction variance given by Eq. (17); the GP modeling has been implemented in MATLAB. Three sets of different mesh refinement combinations are used to train the GP model for the mismatched mesh case, and the results are shown in Table 3.

C. Results and Discussion

We use the finest solution from the no-mismatch case as a benchmark. Note that this solution has not been used to train the error models. For the case of matching meshes, the polynomial model largely overestimated the benchmark value, and the rational function model seems to perform better than the polynomial model for the

Table 3 Comparison of results

Method	Lift (N)
Finest mesh solution (benchmark) ($1/h_{ms} = 12$, $1/h_{fm} = 42$, $1/h_{wm} = 42$)	2019.84
Matching meshes	
Polynomial model	2956.6
Rational function model	1772.9
GP model mean prediction (μ_p)	1993.1
Prediction standard deviation (σ_p)	60.8
Interval for true value ($\mu_p \pm \sigma_p$)	[1932.2,2053.9]
Mismatched meshes: set 1	
Rational function model	2226.6
GP model mean prediction (μ_p)	1948.1
Prediction standard deviation (σ_p)	73.2
Interval for true value ($\mu_p \pm \sigma_p$)	[1874.8,2021.4]
Mismatched meshes: set 2	
Rational function model	1791.7
GP model mean prediction (μ_p)	1929.1
Prediction standard deviation (σ_p)	91.6
Interval for true value ($\mu_p \pm \sigma_p$)	[1837.4,2020.6]
Mismatched meshes: set 3	
Rational function model	2255.8
GP model mean prediction (μ_p)	1929.5
Prediction standard deviation (σ_p)	88.5
Interval for true value ($\mu_p \pm \sigma_p$)	[1841.1,2018.1]

mesh tests considered. For comparison, a GP model was also fit for the matching meshes case. The interval of $\mu_p \pm \sigma_p$ given by the GP model contains the benchmark solution for the case of matching meshes.

As mentioned in Sec. IV, the assumption of asymptotic convergence is difficult to verify in multiple dimensions with mismatching disciplinary meshes. We therefore use only rational function and GP error models for the mismatch case. Table 3 reports the true lift value as predicted by the GP and rational function models for the three sets of mesh refinement combinations considered. As mentioned previously in Sec. V.A, the mesh refinement combinations at which mesh tests are conducted impact the prediction of the true function value. Note that the extrapolation using the rational function model for set 2 is drastically different from those using sets 1 and 3. The impact of mesh refinement combinations is not readily quantifiable for this approach. The advantage of using the GP model is that we can use the prediction variance to estimate bounds on the predicted true solution. These bounds explicitly account for the impact of the mesh refinement combinations that were used to train the error models.

VII. Conclusions

This paper dealt with the estimation of discretization errors in the system output of coupled multidisciplinary systems. Unlike the existing mathematical approaches based on a posteriori methods, an engineering approach for discretization error estimation is proposed in this paper. MDA problems pose unique challenges that make the discretization error quantification challenging. A generic 3-D two-discipline feedback coupled problem is considered. We consider two important effects that contribute to system discretization error, viz., disciplinary meshes and the interface mesh mismatch. Polynomials, rational functions, and Gaussian processes are used as error models. The traditional polynomial and rational function models used for Richardson's extrapolation can pose further challenges for MDA. For polynomial models, the asymptotic convergence assumption is hard to verify for multidimensional and multidisciplinary mesh refinements. For rational functions, it is often ambiguous to choose a functional form. Use of GP models for discretization error is an effective choice. The advantage of the GP model to learn the error model empirically with mesh tests has been illustrated. The GP prediction variance also provides a quantitative measure of the impact of the number and refinement combinations of mesh tests on the predicted true function value. The proposed methods are easily implementable with any commercial finite element codes. A 3-D FSI problem solved in ANSYS has been used as a test case to illustrate the proposed ideas. In future work, the impact of feedback coupling on discretization error of disciplinary inputs/outputs and its impact on discretization and numerical solution errors will be considered. Also, cross-validation schemes can be used to estimate the prediction performance of the error models for mesh tests that were not used in training. Studying the sensitivities of disciplinary and directional mesh refinements on the MDA output will be studied in the future to facilitate resource allocation.

Acknowledgments

This study was supported by funds from NASA Langley Research Center under cooperative agreement no. NNX08AF56A1 (Technical Monitor: Lawrence Green). The support is gratefully acknowledged. Our thanks to Haoxiang Luo of the Department of Mechanical Engineering at Vanderbilt University for his guidance in the ANSYS fluid analysis setup. The computational resources of Vanderbilt University's Advanced Computing Center for Research and Education have been used for the ANSYS simulations in this paper.

References

[1] Nikbay, M., Oncu, L., and Aysan, A., "Multidisciplinary Code Coupling for Analysis and Optimization of Aeroelastic Systems," *Journal of Aircraft*, Vol. 46, No. 6, 2009, pp. 1938–1944. doi:10.2514/1.41491

[2] Martins, J. R. R. A., Alonso, J. J., and Reuther, J. J., "High-Fidelity Aerostructural Design Optimization of a Supersonic Business Jet," *Journal of Aircraft*, Vol. 41, No. 3, 2004, pp. 523–530. doi:10.2514/1.11478

[3] Gamboa, P., Vale, J., Lau, F. J. P., and Suleman, A., "Optimization of a Morphing Wing Based on Coupled Aerodynamic and Structural Constraints," *AIAA Journal*, Vol. 47, No. 9, 2009, pp. 2087–2104. doi:10.2514/1.39016

[4] Rebba, R., Mahadevan, S., and Huang, S., "Validation and Error Estimation of Computational Models," *Reliability Engineering and System Safety*, Vol. 91, Nos. 10–11, 2006, pp. 1390–1397. doi:10.1016/j.ress.2005.11.035

[5] Roache, P. J., *Verification and Validation in Computational Science and Engineering*, Hermosa Publ., Socorro, NM, 1998, pp. 125–128.

[6] Oberkampf, W. L., and Trucano, T. G., "Verification and Validation in Computational Fluid Dynamics," *Progress in Aerospace Sciences*, Vol. 38, No. 3, 2002, pp. 209–272. doi:10.1016/S0376-0421(02)00005-2

[7] Grätsch, T., and Bathe, K.-J., "A Posteriori Error Estimation Techniques In Practical Finite Element Analysis," *Computers and Structures*, Vol. 83, Nos. 4–5, 2005, pp. 235–265. doi:10.1016/j.compstruc.2004.08.011

[8] Ainsworth, M., and Oden, J. T., *A Posteriori Error Estimation in Finite Element Analysis*, Wiley, New York, 2000.

[9] Gratsch, T., and Bathe, K.-J., "Goal-Oriented Error Estimation in the Analysis of Fluid Flows with Structural Interactions," *Computer Methods in Applied Mechanics and Engineering*, Vol. 195, Nos. 41–43, 2006, pp. 5673–5684. doi:10.1016/j.cma.2005.10.020

[10] Richardson, L. F., "The Approximate Arithmetical Solution by Finite Differences of Physical Problems Involving Differential Equations, with an Application of the Stresses in a Masonry Dam," *Philosophical Transactions of the Royal Society of London*, Vol. 210, 1911, pp. 307–357.

[11] Stetter, H. J., *Analysis of Discretization Methods for Ordinary Differential Equations*, Springer Tracts in Natural Philosophy, Springer, New York, 1973, pp. 33–58.

[12] Richards, S. A., "Completed Richardson Extrapolation in Space and Time," *Communications in Numerical Methods in Engineering*, Vol. 13, No. 7, 1997, pp. 573–582. doi:10.1002/(SICI)1099-0887(199707)13:7<573::AID-CNM84>3.0.CO;2-6

[13] Marchi, C. H., and Silva, A. F. C., "Multi-Dimensional Discretization Error Estimation for Convergent Apparent Order," *Journal of the Brazilian Society of Mechanical Sciences and Engineering*, Vol. 27, No. 4, 2005, pp. 432–439. doi:10.1590/S1678-58782005000400012

[14] Soroushian, A., Wriggers, P., and Farjoodi, J., "Asymptotic Upper Bounds for the Errors of Richardson Extrapolation with Practical Application in Approximate Computations," *International Journal for Numerical Methods in Engineering*, Vol. 80, No. 5, 2009, pp. 565–595. doi:10.1002/nme.2642

[15] Dimitrov, S. D., and Kamenski, D. I., "Parameter Estimation in Complicated Rational Functions," *Computers and Chemistry (Oxford) (1976-) / Computers & Chemistry (Oxford)*, Vol. 20, No. 3, 1996, pp. 331–337. doi:10.1016/0097-8485(95)00082-8

[16] Peik, S., Mansour, R., and Chow, Y. L., "Multidimensional Cauchy Method and Adaptive Sampling for an Accurate Microwave Circuit Modeling," *IEEE Transactions on Microwave Theory and Techniques*, Vol. 46, No. 12, 1998, pp. 2364–2371. doi:10.1109/22.739224

[17] Bartkovjak, J., and Karovièová, M., "Approximation by Rational Functions," *Measurement Science Review*, Vol. 1, No. 1, 2001, pp. 63–65.

[18] Stoer, J., and Bulirsch, R., *Introduction to Numerical Analysis*, Springer–Verlag, New York, 1980, pp. 37–143.

[19] Press, W. H., Flannery, B. P., Teukolsky, S. A., and Vetterling, W. T., *Numerical Recipes in FORTRAN 77: The Art of Scientific Computing*, Cambridge Univ. Press, New York, 1992, pp. 167–171.

[20] Kammer, D. C., Alvin, K. F., and Malkus, D. S., "Combining Metamodels with Rational Function Representations of Discretization Error for Uncertainty Quantification," *Computer Methods in Applied Mechanics and Engineering*, Vol. 191, Nos. 13–14, 2002, pp. 1367–1379. doi:10.1016/S0045-7825(01)00328-0

[21] Celik, I., Li, J., Hu, G., and Shaffer, C., "Limitations of Richardson Extrapolation and Some Possible Remedies," *Journal of Fluids Engineering*, Vol. 127, No. 4, 2005, pp. 795–806.

doi:10.1115/1.1949646
[22] *ANSYS Coupled Field Analysis Guide: ANSYS Release 11*, ANSYS, Inc., Canonsburg, PA, 2007.
[23] Ghattas, O., and Li, X., "A Variational Finite Element Method for Stationary Nonlinear Fluid–Solid Interaction," *Journal of Computational Physics*, Vol. 121, No. 2, 1995, pp. 347–356. doi:10.1016/S0021-9991(95)90204-X
[24] Michler, C., van Brummelen, E. H., Hulschoff, S. J., and de Borst, R., "The Relevance of Conservation for Stability and Accuracy of Numerical Methods for Fluid–Structure Interaction," *Computer Methods in Applied Mechanics and Engineering*, Vol. 192, Nos. 37–38, 2003, pp. 4195–4215. doi:10.1016/S0045-7825(03)00392-X
[25] Felippa, C. A., Park, K. C., and Farhat, C., "Partitioned Analysis of Coupled Mechanical Systems," *Computer Methods in Applied Mechanics and Engineering*, Vol. 190, Nos. 24–25, 2001, pp. 3247–3270. doi:10.1016/S0045-7825(00)00391-1
[26] Kim, H.-G., "Interface Element Method (IEM) for a Partitioned System with Non-Matching Interfaces," *Computer Methods in Applied Mechanics and Engineering*, Vol. 191, Nos. 29–30, 2002, pp. 3165–3194. doi:10.1016/S0045-7825(02)00255-4
[27] Maman, N., and Farhat, C., "Matching Fluid and Structure Meshes for Aeroelastic Computations: A Parallel Approach," *Computers and Structures*, Vol. 54, No. 4, 1995, pp. 779–785. doi:10.1016/0045-7949(94)00359-B
[28] Jiao, X., and Heath, M. T., "Common-Refinement-Based Data Transfer Between Non-Matching Meshes in Multiphysics Simulations," *International Journal for Numerical Methods in Engineering*, Vol. 61, No. 14, 2004, pp. 2402–2427. doi:10.1002/nme.1147
[29] Jaiman, R. K., Jio, X., Geubelle, P., and Loth, E., "Conservative Load Transfer Along Curved Fluid–Solid Interface with Non-Matching Meshes," *Journal of Computational Physics*, Vol. 218, No. 1, 2006, pp. 372–397. doi:10.1016/j.jcp.2006.02.016
[30] Jaiman, R. K., Jio, X., Geubelle, P., and Loth, E., "Assessment of Conservative Load Transfer for Fluid–Solid Interface with Non-Matching Meshes," *International Journal for Numerical Methods in Engineering*, Vol. 64, No. 15, 2005, pp. 2014–2038. doi:10.1002/nme.1434
[31] Alexandrov, N. M., and Lewis, R. M., "Algorithmic Perspectives on Problem Formulation in MDO," 8th AIAA/USAF/NASA/ISSMO Symposium on Multidisciplinary Analysis and Optimization, Long Beach CA, AIAA Paper 2000-4719, 2000.
[32] Keane, A. J., and Nair, P. B., *Computational Approaches for Aerospace Design: The Pursuit of Excellence*, Wiley, New York, 2005, pp. 359–385.
[33] Alexandrov, N. M., and Lewis, R. M., "Analytical and Computational Aspects of Collaborative Optimization for Multidisciplinary Design," *AIAA Journal*, Vol. 40, No. 2, 2002, pp. 301–309. doi:10.2514/2.1646
[34] Sobieszczanski-Sobieski, J., and Haftka, R. T., "Multidisciplinary Aerospace Design Optimization: Survey of Recent Developments," *Structural optimization*, Vol. 14, No. 1, 1997, pp. 1–23. doi:10.1007/BF01197554
[35] Tedford, N. P., and Martins, J. R. R. A., "Benchmarking Multidisciplinary Design Optimization Algorithms," *Optimization and Engineering*, Vol. 11, No. 1, 2009, pp. 159–183. doi:10.1007/s11081-009-9082-6
[36] Farhat, C., Lesoinne, M., and Le Tallec, P., "Load and Motion Transfer Algorithms for Fluid/Structure Interaction Problems with Non-Matching Discrete Interfaces: Momentum and Energy Conservation, Optimal Discretization and Application to Aeroelasticity," *Computer Methods in Applied Mechanics and Engineering*, Vol. 157, Nos. 1–2, 1998, pp. 95–114. doi:10.1016/S0045-7825(97)00216-8
[37] Rasmussen, C. E., and Williams, C. K. I., *Gaussian Processes for Machine Learning*, Springer, New York, 2006.
[38] Heiser, R. F., and Parrish, W. R., "Representing Physical Data with Rational Functions," *Industrial and Engineering Chemistry Research*, Vol. 28, No. 4, 1989, pp. 484–489. doi:10.1021/ie00088a017
[39] Dohrmann, C. R., Key, S. W., and Heinstein, M. W., "A Method for Connecting Dissimilar Finite Element Meshes in Two Dimensions," *International Journal for Numerical Methods in Engineering*, Vol. 48, No. 5, 2000, pp. 655–678. doi:10.1002/(SICI)1097-0207(20000620)48:5<655::AID-NME893>3.0.CO;2-D
[40] Maute, K., Nikbay, M., and Farhat, C., "Coupled Analytical Sensitivity Analysis and Optimization of Three-Dimensional Nonlinear Aeroelastic Systems," *AIAA Journal*, Vol. 39, No. 11, 2001, pp. 2051–2061. doi:10.2514/2.1227
[41] Holmström, K., Edvall, M. M., and Göran, A. O., "TOMLAB: For Large-Scale Robust Optimization," *Proceedings of the Nordic MATLAB Conference*, 2003, pp. 218–222.

A. Messac
Associate Editor